Engineering Science and Technology, an International Journal 27 (2022) 101017

Contents lists available at ScienceDirect

Engineering Science and Technology, an International Journal

journal homepage: www.elsevier.com/locate/jestch

Full Length Article

Dielectric properties, electric modulus and conductivity profiles of Al/Al_2O_3/p-Si type MOS capacitor in large frequency and bias interval

Serhat Orkun Tan [a,*], Osman Çiçek [b], Çağrı Gökhan Türk [c], Şemsettin Altındal [d]

[a] Karabük University Department of Electrical Engineering, 78050, Karabuk, Turkey
[b] Kastamonu University, Department of Electrical and Electronics Engineering Kastamonu 37150 Turkey
[c] Gazi University, Department of Metallurgy and Material Science Engineering Ankara, Turkey
[d] Gazi University, Faculty of Sciences, Department of Physics, Ankara, Turkey

ARTICLE INFO

Article history:
Received 10 February 2021
Revised 27 April 2021
Accepted 26 May 2021
Available online 09 June 2021

Keywords:
Frequency dependence
Dielectric properties
Electric modulus
Surface states
Polarization
Conductivity

ABSTRACT

The letter reports that the impedance spectroscopy method has been performed to acquire impeccable results on the ac electric conductivity (σ_{ac}), dielectric (ε' and ε'') and electric modulus (M' and M'') components of the Al/Al_2O_3/p-Si type MOS capacitor. The relevant parameters are defined with C-V-f and G/ω-V-f data between 1 kHz and 5 MHz and ± 3 V at room temperature. Both parts of dielectric constants are decreasing at high frequencies to prevent the interface dipoles from gaining enough time to return to the alternative area. Depending on the restructuring and reorganization of surface states (N_{ss}) in the alternative field, tanδ decreases at higher frequencies. The M' values reach maximum by frequency increment in the depletion region, while M'' values shift to the forward biases depending on a certain density distribution of N_{ss}. The σ_{ac} values increase with increasing frequency in the accumulation region depending on series resistance. Considering polarization processes, surface conditions (N_{ss}) and Al_2O_3 interlayer, frequency and biases are extremely effective and dependent on the dielectric specifications, electrical modulus and conductivity.

© 2021 Karabuk University. Publishing services by Elsevier B.V. This is an open access article under the CC BY-NC-ND license (http://creativecommons.org/licenses/by-nc-nd/4.0/).

1. Introduction

The transformation of metal–semiconductor (MS) type structures into metal-insulator-semiconductor (MIS) or metal- oxide-semiconductor (MOS) structures take place thanks to many different methods such as thermal oxidation, sputtering and ALD, which allows adding an oxide layer to the MS interface [1–5]. However, the used such a high-dielectric can be improved the diode parameters performance such as the reduction in R_s, leakage current, N_{ss} and the increment in the capacitance, storage energy or charges [6–8]. Although being compatible with Si wafer provides an advantage to SiO_2 in terms of good gate dielectrics, having low dielectric constant of $3.8\varepsilon_o$ is a disadvantage for it. This adverse condition poses a problem on preventing inadmissible high N_{ss} or dislocations between the interlayer and semiconductor. Accordingly, many high dielectric materials such as Al_2O_3, Sm_2O_3, polystyrene/TiO_2, 7% graphene doped-PVA, $BaTiO_3$ have been used by the researchers at MS interface to improve the electric and dielectric qualifications of MIS type devices. Together with frequency and applied bias across the device, interlayer's homogeneity, and thickness and also semiconductor's surface preparation has influenced the conduction mechanisms and performance of the structure [11].

Including capacitance and conductance (C and G/ω) measured at any frequency, impedance changes are dependent on the ability of electron concentration's ac signal tracking, polarization processes, and external dc bias or electric field as well as temperature. The electrons captured by surface states/interface traps (N_{ss}/D_{it}) can trace this alternating current only at low frequencies. In this way, it can give an excess C and G/ω which depend on the angular frequency and lifetime (τ) of the traps [4,5,11]. Besides *M'* and *M''* and σ_{ac}, dielectric characteristic of MIS type structure or capacitors are also strongly dependent of N_{ss}, R_s, interfacial layer, frequency, voltage, and polarization processes. On the other hand, impedance measurements solely at confined frequency and bias interval cannot provide more accuracy and reliable results both on the electric and dielectric specifications of MIS type electronic devices. Contrary, when these measured at large frequency and bias interval, more detailed information can be achieved on electrical and dielectric properties [12,13].

* Corresponding author at: Karabük University Department of Electrical Engineering, 78050, Karabuk, Turkey.

E-mail addresses: serhatorkuntan@karabuk.edu.tr (S.O. Tan), ocicek@kastamonu.edu.tr (O. Çiçek), turkcagrigokhan@gmail.com (Ç.G Türk), altundal@gazi.edu.tr (Ş. Altındal).

Peer review under responsibility of Karabuk University.

https://doi.org/10.1016/j.jestch.2021.05.021
2215-0986/© 2021 Karabuk University. Publishing services by Elsevier B.V.
This is an open access article under the CC BY-NC-ND license (http://creativecommons.org/licenses/by-nc-nd/4.0/).

The alteration in dielectric and electric modulus parameters by frequency are usually the result of relaxation processes and N_{ss} at low and moderate frequencies as for the electric dipoles have time to align with the field before it alters its pointing and N_{ss} is able to track an external alternating current (ac) signal; consequently, ε' and ε'' are considerably high. But, at high frequencies, ε' and ε'' decreases due to shorter time available for the dipoles to align and effect of R_s [14]. The observed high-dielectric constant (=8.5) even at 1 kHz for the used Al_2O_3 is an evident to these phenomena. In addition, capacitor storing electric charges and so electrical energy is a basic circuit component and the higher capacitance can be achieved by used a high dielectric interlayer with low thickness. The other important point is to extract as much information as possible, dielectric relaxation phenomena, electric modulus and conductivity mechanisms impedance measurements should be performed in wide range of frequency and voltage [9].

Due to above explanations, in this study, we aimed to investigate complex dielectric constant (ε^*) and complex modulus of the fabricated Al/*p*-Si (MS) with Al_2O_3 interlayer deposited by ALD. For this aim, at room temperature conditions, impedance measurements were completed between 1 kHz and 5 MHz and ± 3 V to acquire meticulous and steady results on these parameters as well as conductivity. Hereby, experimental results have revealed that, N_{ss}, external electric field, and the interfacial and dipole polarization are more effective on the dielectric specifications, electrical modulus, and conductivity remarkably at low frequencies and in depletion layer.

2. Experimental Details

Al/Al_2O_3/p-Si type MOS capacitor was produced on Boron-doped *p*-Si with 300 μm thickness, 100 surface orientation and 1.39×10^{16} cm^{-3} doping acceptor atoms (NA). First of all, *p*-Si wafer was cleaned in an ultrasonic bath utilizing distinct chemical solutions. Following this cleaning, highly resistant deionized water (DI) was used for washing and N_2 gas was used for drying.

In the next step, Al with 99.999% pure and 150 nm thickness was coated on the *p*-Si backside at 10^{-6} Torr. Annealing was carried out in nitrogen atmosphere at 550 °C to acquire a low resistivity and pre-eminent ohmic contact. Finally, utilizing the ALD method, Si wafer was deposited with the Al_2O_3 interlayer. Right after Al_2O_3 deposition, almost completely pure Al dots with 0,5 mm radius and 150 nm thicknesses, were thermally evaporated on the deposited layer's forepart at 10^{-6} Torr by the aid of a shadow mask.

The HP-4192 A LF impedance analyzer was preferred to perform conductance and capacitance measurements was operated at −3V to +3 V biases and 1 kHz to 5 MHz frequencies interval. The usage of analyzer was accompanied by a microcomputer operated via the IEEE-488 AC/DC converter board during measurements. The experimental setup is given below in Fig. 1 and in terms of detailed information, our previous study, which includes the diagram of the samples and the fabrication processes can be examined [15].

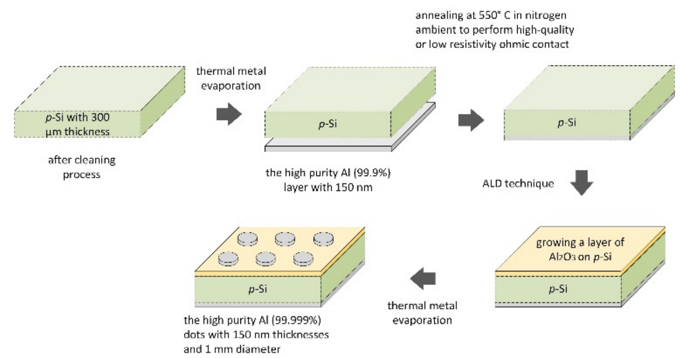

Fig. 1. The schematic diagram for experimental setup.

3. Results and Discussion

The capacitance occurs in the existence of an organic/polymer or inorganic insulator between semiconductor and metal. Capacitance depends on the N_{ss} between the insulator and semiconductor, and therefore the dielectric properties of the insulating layer. In the structures, the electrical equivalent circuit model including the effect of the N_{ss} is expressed in Fig. 2a [4]. Here, the *Ci/Cox* is the capacitance of the insulating layer, while the C and G are the frequency-dependent C and G/ω, respectively.

To explain the dielectric properties of Al/Al_2O_3/*p*-Si type MOS capacitor, their C and G/ω characteristics are obtained in the wide-ranged frequencies (1 kHz to 5000 kHz) and also, given in Fig. 2b and c, respectively. It can be clearly seen that the C and G/ω values depending on the applied voltage increase with the increasing frequency. In the MS structures, as an organic/polymer or inorganic insulator inserted between M and S, the sensitivity of the insulator layer with respect to the applied electrical field is obtained by examining the dielectric properties. The admittance (Y) is expressed by $Y = G + j\omega C$ based on the circuit model given in Fig. 2a [5,16,17]. Assuming the dielectric material is an air gap, the capacitance of the device is C_0 and the relative dielectric permittivity is ε^*. The above equation is expressed as $Y = G + j\omega(C_0\varepsilon^*)$. Furthermore, when the ε^* is written in fixed polar coordinate [17,18]:

$$\varepsilon^* = \varepsilon' - j\varepsilon'' = \frac{C}{C_0} - j\frac{G}{\omega C_0} \quad (1)$$

Using the C and G values of Al/Al_2O_3/*p*-Si type MOS capacitor, ε' *and* ε'' values at variable frequencies were calculated by the following equations [5]:

$$\varepsilon' = \frac{C}{C_0} = j\frac{Cd_{ox}}{\varepsilon_0 A} \quad (2)$$

$$\varepsilon'' = \frac{G}{\omega C_0} = \frac{Gd_{ox}}{\varepsilon_0 \omega A} \quad (3)$$

where, A is the contact area (cm^2), d_{ox} is the isolated layer thickness, ε_0 is the dielectric constant equals to $8{,}85\cdot10^{-14}$ F/cm. The C_i/C_{ox} value of the insulator layer for the structure was obtained from the strong accumulation region and also, is expressed by. Using the Eqs. (2) and (3), $tan\delta$ can be expressed as following [19]:

$$\tan\delta = \frac{\varepsilon''}{\varepsilon'} \quad (4)$$

In Fig. 3, the voltage-dependent dielectric characteristics of the MOS capacitor structure for variable frequencies are explained. Here, the ε' values increase with increasing the applied biases in the depletion and accumulation regions, as they are static in the inversion region (Fig. 3a). In addition, the ε' values at low frequencies especially increase in the depletion regions, while these values decrease with increasing frequency. This is attributed to N_{ss} and dipole polarization. Similarly, the ε'' values give a peak in the depletion region, around −1 V to −0.5 V, at low frequencies (≤100 kHz) due to the limited number of majority carriers located between the bandgap. These peaks shift from reverse bias voltage to forward bias voltage (Fig. 3b). As a result of the previously mentioned N_{ss} and ac signal relation, while N_{ss} and polarization are dominated especially in the depletion region at low and moderate frequencies due to easy respond to external ac-signal, R_s is domi-

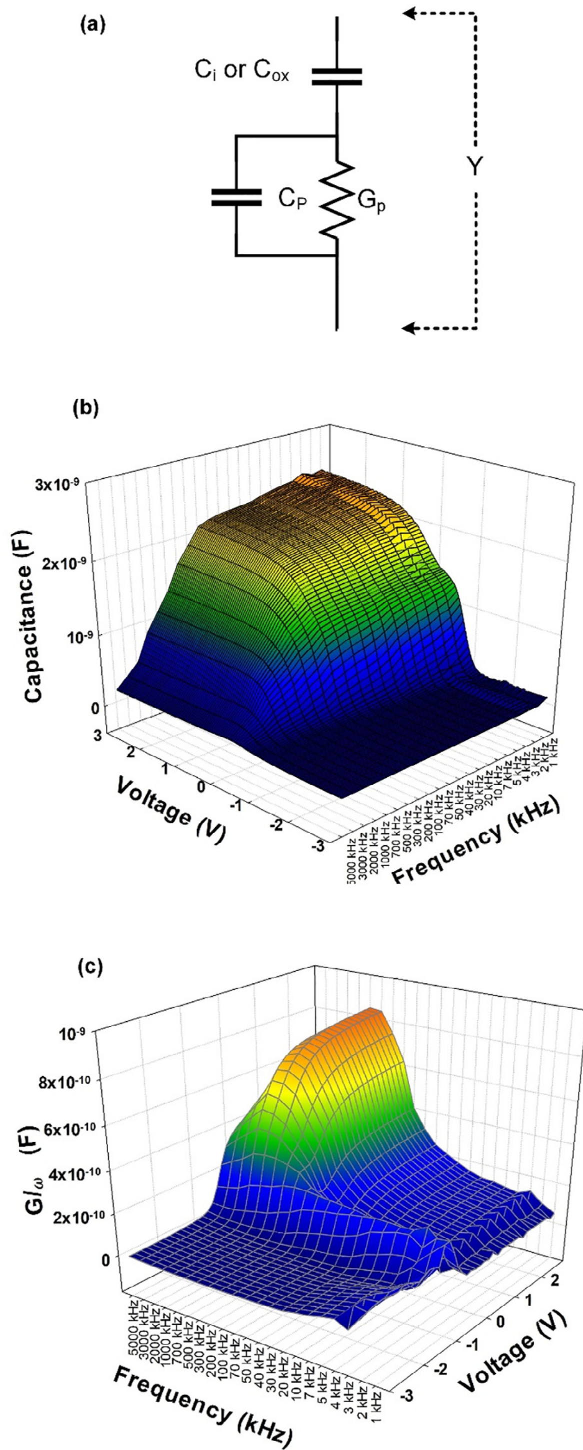

Fig. 2. (a) The electrical equivalent circuit model, (b), (c) the frequency-dependent C and G/ω graphs of Al/p-Si structure with Al_2O_3 thin-film insulating layer.

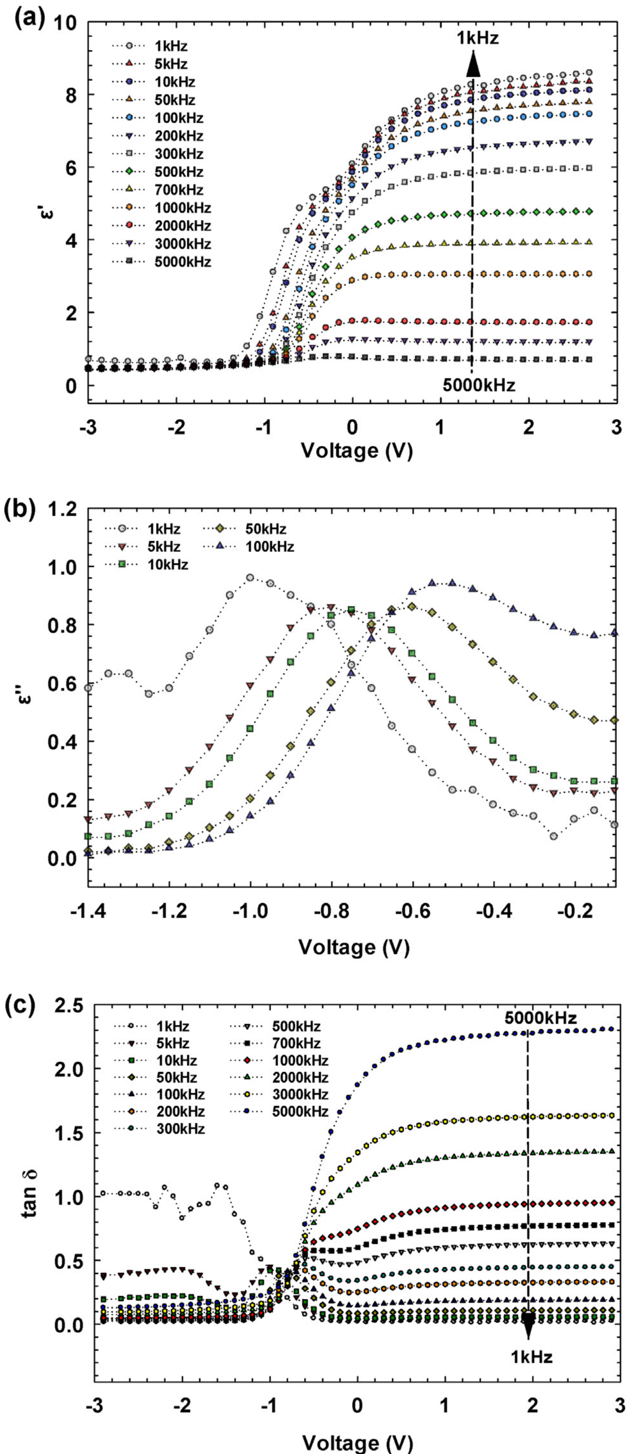

Fig. 3. The voltage-dependent profile of the a) reel dielectric constant, b) imaginary dielectric constant, c) loss tangent.

nated only at accumulation region at high frequencies [6,9,10]. Furthermore, the *tanδ* values appear to be significantly dependent on voltage and frequency (Fig. 3c). It is confirmed that the N_{ss} and interfacial polarization on the *tanδ* values at variable frequencies are effective in the inversion regions, while R_s and the insulator layer on them are effective in the accumulation region.

The grown of low-dielectric insulator interlayer such as SiO_2 by traditional-methods, such as thermal and wet oxidation, at M/S interface cannot passivate as entirely the active dangling-bonds at semiconductor's surface. Therefore, in recently, researchers are focused on the improving the performance of the MS structures by using some high-dielectric insulator layer at M/S interface such as Al_2O_3, TiO_2, metal-oxide instead of conventional SiO_2. Therefore, high dielectric material is necessary to produce a high-capacitor and it can be used in a wide range of charge/energy storage applications [20,21].

Furthermore, the ac conductivity $\sigma_{ac}(\omega)$ can be obtained from the following equation [22]:

$$\sigma_{ac}(\omega) = \varepsilon''\omega\varepsilon_0 = \varepsilon''(2\pi f)\varepsilon_0 \quad (5)$$

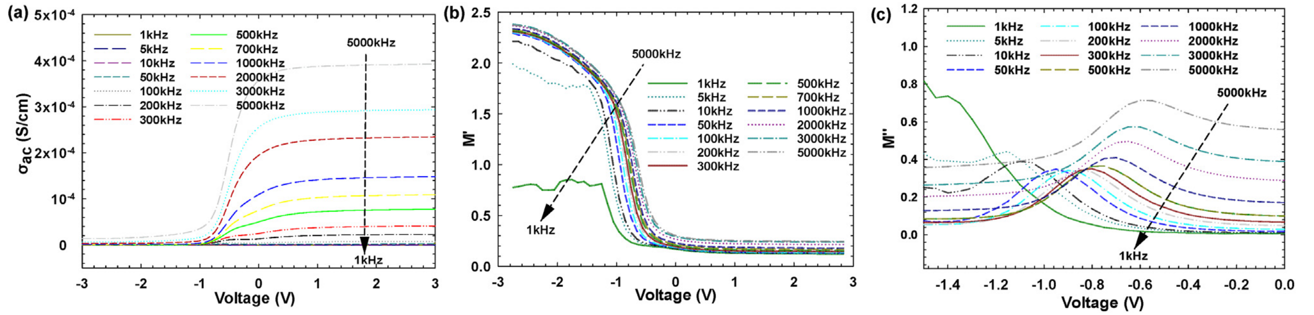

Fig. 4. a) The voltage-dependent σac, b) the real and c) imaginary modulus parts of the structure.

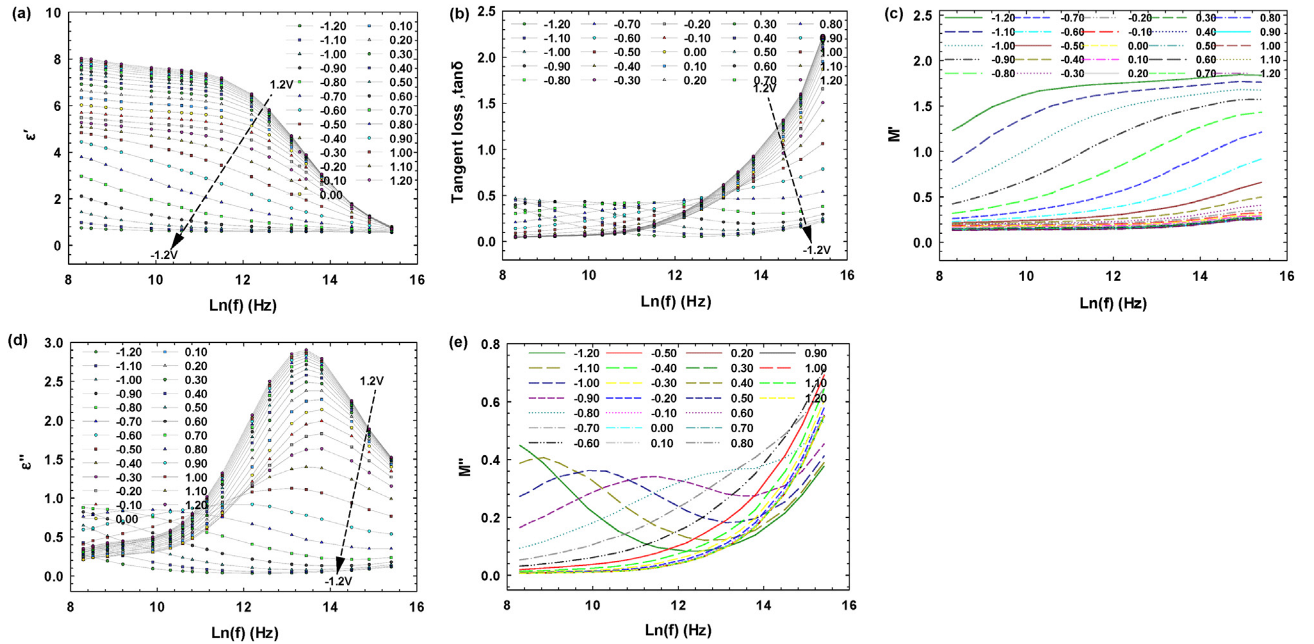

Fig. 5. The frequency-dependent graphs of all related parameters components for MOS capacitor.

Using the Eq. (5), the voltage-dependent σ_{ac} values are calculated for each frequency and given in Fig. 4a. While σ_{ac} is almost independent from frequency in inversion region, it suddenly becomes increase in depletion region due to the existence of surface states especially at low and moderate frequencies and then shows a saturate behaviour at accumulation region due to the effect of R_s. The independent frequency behaviour of σ at low and moderate frequencies corresponding to the direct current (dc) conductivity, but at high frequencies it corresponds to the ac conductivity. This condition is attributed to the R_s [23,24]. When R_s is effective only at accumulation region at high frequencies, N_{ss} are effective both in depletion and weak inversion regions at low and intermediate frequency ranges. Therefore, the decrease of R_s with increasing frequency leads to an increase in conductance ($G = 1/R_s$) or σ_{ac} at accumulation region. Thus, imaginary dielectric constant value ($\varepsilon''=(G/\omega C_o)$) and so loss-tangent ($tan\delta = \varepsilon''/\varepsilon$) are also increase with increasing frequency at accumulation region. The existence of R_s may be caused some errors in the extraction of electric or dielectric properties and to avoid these errors, R_s can be minimized by (1) sample fabrication, (2) making measurements at low-intermediate frequencies, and (3) measuring R_s and applying a correction to the measured C/G-V before the desired information is extracted. On the other hand, the observed peak in the ε'' vs V plot in depletion region at low and intermediate frequencies is the result of a special density distribution of N_{ss} located in the band gap of semiconductor at interface as randomly.

The components of the complex electric modulus (M^*) based on ε^* are separated into the real (M') and imaginary (M'') components as following [25]:

$$M^* = \frac{1}{\varepsilon^*} = M' + jM'' = \frac{\varepsilon'}{(\varepsilon')^2 + (\varepsilon'')^2} + j\frac{\varepsilon''}{(\varepsilon')^2 + (\varepsilon'')^2} \quad (6)$$

Using the Eq. (6), the voltage-dependent M' and M'' values in the wide-ranged frequency are calculated and expressed in Fig. 4b and c. Here, it is seen that the M' and M'' values significantly depend on frequency. Also, depending on the frequency, M'' values peak in the depletion region and reach their maximum values with the increasing frequency.

On the other hand, the M'' values peak in the voltage ranged −1.5 V to 0 V owing to a particular density distribution of N_{ss} and their relaxation times, and their positions shift towards forward bias region with increasing frequency.

Frequency-dependent graphs of all related parameters of the structure are explained in Fig. 5. Dielectric parameters as constants

and loss tangent vary depending on the biases at low frequencies, on the other hand this dependency disappears at high frequencies. Because the contribution of interface and dipolar or ionic polarization to the ε', ε'' and N_{ss} at increasing frequencies is ineffective. The decrease in the ε' and ε'' values with increasing frequency can be explained as follows; since the frequency is increased, the interface dipoles have less time to orient towards the alternative field [26].

Obviously, the dielectric parameters values at high frequencies are close to each other. *Tanδ-logf* values give peaks at Fig. 5c and this peak size decreases with increasing applied biases and peaks are shifting towards high frequency. Such frequency-dependent behavior of *tanδ* can be attributed to the reconstruction and reordering of interface states under the alternative field.

4. Conclusions

Dielectric qualifications, electric modulus, and conductivity profiles for the fabricated Al_2O_3 interlayered Al/*p*-Si structure were identified through C-V-f and G/ω-V-f data at wide frequency range (1kHz–5000 kHz) under ordinary room temperature conditions. It is clear that C and G/ω values increase with increasing frequency depending on the applied biases. While ε' values decrease with increasing frequency, they increase especially in depletion regions due to N_{ss} and dipole polarization at low frequencies. Similarly, ε'' values give a peak in the depletion region at low frequencies caused by a limited number of majority carriers. The effect of bias and frequency is seen significantly on the *tanδ* values in the regions of inversion and accumulation. Depending on R_s, σ_{ac} values increase with increasing frequency in the accumulation region. *M'* values reach their maximum with frequency increment in the depletion region. The position of *M''* values shift towards the forward biases with increasing frequency due to a certain density distribution of N_{ss}. and relaxation times. The decrement in ε' and ε'' values at high frequencies is due to the fact that frequency increment prevents to gain adequate time for the interface dipoles to turn to the alternative field. As clearly seen, both parts of the dielectric constants at high frequencies are close to each other. The peaks at tanδ-logf graph are decreasing with increasing biases and shifting towards high frequencies. This frequency-dependent behaviour of *tanδ* can be associated with the restructuring and reorganization of N_{ss} in the alternative field.

Declaration of Competing Interest

The authors declare that they have no known competing financial interests or personal relationships that could have appeared to influence the work reported in this paper.

Acknowledgements

This study was supported by Gazi University Scientific Research Project. (Project Number: GU-BAP.05/2019-26).

References

[1] M. Sharma, S.K. Tripathi, J. Appl. Phys. 112 (2012) 024521.
[2] S.O. Tan, H.U. Tecimer, O. Çiçek, IEEE Trans. Electron Devices 64 (3) (2017) 984–990.
[3] S.O. Tan, IEEE Trans. Nanotechnol. 18 (2019) 432–436.
[4] E.H. Nicollian, MOS (Metal Oxide Semiconductor) Physics and Technology, Wiley-Interscience, 2002.
[5] S.M. Sze, Physics of Semiconductor Devices, 2 ed., Willey, New York, 1981.
[6] L. Kankate, C. Nies, W. Possart, H. Kliem, IEEE Trans. Dielectr. Electr. Insul. 25 (4) (2018) 1508–1517.
[7] V. Manjunath, V.R. Reddy, S.P.R. Reddy, V. Janardhanam, C.J. Choi, Curr. Appl. Phys. 17 (2017) 980–988.
[8] A.A. Gulyakova, Y.A. Gorokhovatsky, P. Frübing, R. Gerhard, IEEE Trans. Dielectr. Electr. Insul. 24 (4) (2017) 2541–2548.
[9] S. Altındal Yerişkin, M. Balbaşı, A. Tataroğlu, J. Appl. Polym. Sci. 133 (2016) 43827.
[10] V.R. Reddy, V. Manjunath, V. Janardhanam, Y.-H. Kil, C.-J. Choi, J. Electron. Mater. 43 (2014) 3499.
[11] H. Card, E. Rhoderick, J. Phys. D Appl. Phys. 4 (1971) 1589–1601.
[12] A. Kaya, Ş. Altındal, Y.Ş. Asar, Z. Sönmez, Chin. Phys. Lett. 30 (2013) 017301.
[13] C.P. Symth, Dielectric Behaviour and Structure, McGraw-Hill, New York, 1995.
[14] H.N. Chandrakala, B. Ramaraj, G.M. Madhu, J. Mater. Sci. 47 (2012) 8076–8084.
[15] Ç.G. Türk, S.O. Tan, Ş. Altındal, B. İnem, Phys. B Condens. Matter 582 (2020) 411979.
[16] O. Cicek, IEEE Trans. Nanotechnol. 19 (2020) 172–178.
[17] C.A. Wert, R.M. Thomson, Physics of Solids, 2nd ed., McGraw-Hill, New York, 1970.
[18] V.V. Daniel, Dielectric Relaxation, Academic Press, London, 1967.
[19] A.R. Von Hippel, Dielectrics and Waves, John Wiley & Sons, New York, 1959.
[20] H.G. Çetinkaya, Ö. Sevgili, Ş. Altındal, Phys. B Condens. Matter. 560 (2019) 91–96.
[21] S. Karadaş, S. Altındal Yerişkin, M. Balbaşı, Y. Azizian-Kalandaragh, J. Phys. Chem. Solids 148 (2021) 109740.
[22] P. Pissis, A. Kiritsis, Solid-State Ion 97 (1997) 105.
[23] O. Pakma, N. Serin, T. Serin, Ş. Altındal, J. Phys. D: Appl. Phys. 41 (2008) 215103.
[24] S.P. Szu, C.Y. Lin, Mater. Chem. Phys. 82 (2) (2003) 295–300.
[25] M.D. Migahed, M. Ishra, T. Fahmy, A. Barakat, J. Phys. Chem. Solids 65 (6) (2004) 1121–1125.
[26] M.H. Al-Dharob, A. Kökce, D.A. Aldemir, A.F. Özdemir, Ş. Altındal, J. Phys. Chem. Solids 144 (2020) 109523.